

IMAGE PROCESSING

PACS numbers: 42.30.Va; 42.65.Jx
DOI: 10.1070/QE2011v041n06ABEH014605

Self-imaging of transparent objects and structures in focusing of spatially phase-modulated laser radiation into a weakly absorbing medium*

E.L. Bubis

Abstract. **Self-imaging of transparent objects and structures in focusing of a spatially phase-modulated laser beam into an extended weakly absorbing medium is described. The laser power level that is necessary for effective imaging corresponds to the illuminating beam power when thermal self-defocusing starts evolving in the medium. The effect can be described in terms of the ideology of Zernike's classical phase-contrast method. Edge enhancement in visualised images of transparent objects is experimentally demonstrated. Self-imaging of a microscopic object in the form of transparent letters and long-lived refractive-index fluctuations in liquid glycerol is shown. Due to the adaptivity of the process under consideration, unlike the classical case, self-imaging occurs also in the situations where a beam is displaced (undergoes random walk) as a whole in the Fourier plane, for example, in the presence of thermal flows.**

Keywords: *Zernike phase-contrast method, nonlinear optics, laser beam thermal self-action.*

The classical phase-contrast method is widely used to observe (visualise) transparent localised objects and structures [1 – 6]. To transform the phase modulation that is introduced by the object studied into the illuminating beam into amplitude modulation, a phase screen (Zernike filter) is installed in the focal objective (Fourier) plane. This screen introduces a selective phase shift $\theta = \pm\pi/2$ between zero and higher spatial harmonics that are involved in the formation of the object image. In the nonlinear phase-contrast method spatial frequencies are misphased in a cubically nonlinear medium (nonlinear Zernike filter), the medium being also located in the Fourier plane, where the spatial harmonics are separated [4, 7 – 16]. In comparison with the schemes applying linear Zernike cells, this is a more flexible adaptive scheme, where the necessary phase shift is obtained by choosing the corresponding light intensity at the input of the nonlinear medium.

Phase objects in schemes with thin photothermal filters were imaged in [9 – 14]. Here, we report self-imaging of transparent objects that is based on the thermal mechanism of nonlinearity, in a scheme with an extended (optically thick) weakly absorbing medium. The latter not only decreases the laser power that is necessary to misphase spatial frequencies but also makes the process completely adaptive, i.e., independent of neither the angle of incidence of the illuminating beam nor the position of the focal region in the medium. This is especially important for imaging of large phase objects, whose sizes are comparable with the illuminating-beam diameter, and in the case of beam random walk in the Fourier region. An effective transformation of phase modulation, in combination with a good quality of a visualised image of a transparent structure occurs in a narrow range of illuminating beam powers. It is no doubt that the self-imaging during propagation of light beams in weakly absorbing extended media is a new effect. In the region of small thermal changes in the refractive index of the medium, the nonlinear phase delay is insufficient to implement the desired phase mismatch ($\theta = \pm\pi/2$) and, therefore, effective self-imaging. At large nonlinear phase delays the visualised image quality is deteriorated because of strong thermal self-action of the laser beam illuminating a transparent object in the medium. By analogy with self-action this effect can be referred to as self-imaging. When propagating in a weakly absorbing medium, the beam that is focused in it changes the phase relations between the spatial harmonics involved in the image formation, as a result of which the phase inhomogeneities (structures) present in the beam are effectively imaged at a certain beam power (energy). The imaging settling time τ is determined from the relation $\tau \approx d^2/4\chi$, where d is the maximum diameter of the heating beam in the medium and χ is the thermal diffusivity, which is equal, for example, to $\sim 1.5\times 10^{-3}$ cm^2 s^{-1} for water and $\sim 2\times 10^{-1}$ cm^2 s^{-1} for air.

When technological lasers are used, the transformation of phase modulation into amplitude can also be a minor (accompanying the thermal-lens formation) negative effect, which accentuates the inhomogeneities in the wavefront of the initial beam and additionally deteriorates it in the plane of the object processed due to the nonlinearity of the channel through which radiation passes.

The scheme of the effect observation is shown in Fig. 1. It is based on a simple single-lens system of image formation with a photothermal cell located in the Fourier plane of the system. An absorbing medium can occupy the entire space between the objective and image plane.

The transparent objects located in the object plane were illuminated by a Gaussian linearly polarised beam of a

* Reported at the conference 'Laser Optics', Russia, St. Petersburg, June 2010.

E.L. Bubis Institute of Applied Physics, Russian Academy of Sciences, ul. Ul'yanova 46, 603950 Nizhnii Novgorod, Russia;
e-mail: bel@appl.sci-nnov.ru

Received 25 February 2011
Kvantovaya Elektronika **41** (6) 568 – 570 (2011)
Translated by Yu.P. Sin'kov

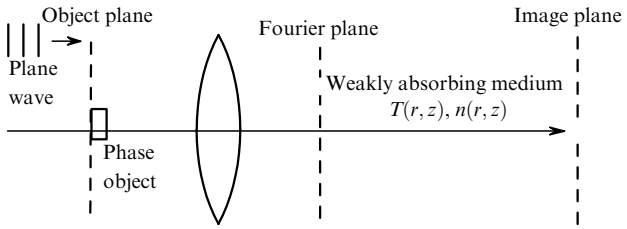

Figure 1. Scheme for observing the self-imaging effect [($T(r,z)$ and $n(r,z)$ are, respectively, the temperature and refractive index distributions in the medium].

single-mode He–Ne laser with a power $P \leqslant 6$ mW and the wavelength $\lambda = 0.63$ μm or by a beam of a green laser pointer with $\lambda = 0.53$ μm and $P \leqslant 30$ mW. The beam power was controlled by rotating a Glan prism (not shown in Fig. 1) around its axis and measured by an IMO-2M calorimeter. The radiation transmitted through the object was focused by the lens in the middle of the cell, which was filled with ethyl alcohol or water, with absorbent added.

The absorption losses were chosen to satisfy the condition $\alpha l \approx 0.2 - 0.6$ (α is the absorption coefficient of the medium and l is the cell length). We used cells with lengths $l = 1 - 300$ mm. The transparent objects under study were imaged on a screen located in the image plane at a distance up to 10 m from the lens and recorded by a digital camera or (in the direct beam) by a camera without an objective.

According to [2], in a phase-contrast system containing a phase object, which introduces a small local phase shift $\varphi(x,y) < 1$ into the plane wave, the light intensity distribution in the image plane at the phase shift θ between zero and higher spatial harmonics has the form

$$I_{\text{out}} \propto [1 + 2\varphi(x,y)\sin\theta]. \tag{1}$$

It follows from (1) that small phase delays in the object plane are linearly transformed into intensity changes in the image plane. Depending on the phase sign, there may be either positive (bright) or negative (dark) contrast. At large phase shifts the linearity is disturbed; however, transparent objects are nevertheless imaged.

Let us perform simple estimation of the energy (in case of time-dependent illumination) and power (in case of continuous illumination) at which the effect can be observed.

A single-mode light beam with an energy E, focused into an optically thick (infinite), weakly absorbing medium, acquires an additional phase shift due to the heating of the medium in the time-dependent case:

$$\theta = 2\pi \frac{E}{E_{\text{cr}}},$$

where

$$E_{\text{cr}} = \frac{2\pi\rho c_p}{\alpha k^2 (\partial n/\partial T)_p}$$

is the critical thermal self-action energy (see, for example, [17]); ρ is the density of the medium; c_p is its specific heat at a constant pressure; $k = 2\pi/\lambda$ is the wave number; and $(\partial n/\partial T)_p$ is the temperature derivative of the refractive index (at a constant pressure). For water in the visible spectral range, at $\alpha \approx 10^{-3} - 10^{-4}$ cm^{-1}, the necessary energy is several tens of millijoules. In the time-dependent case the phase shift for a rectangular pulse is a linear function of time, and the required value $\theta = \pi/2$ is reached only by the end of the pulse.

Under continuous illumination the necessary power P is estimated from the relation [18, 19]

$$\theta = \frac{\pi}{2} = \frac{\alpha l P}{\varkappa\lambda(\partial n/\partial T)},$$

where $\varkappa$ is the thermal conductivity of the medium. Using the tabulated data and assuming that $\alpha l \approx 0.3$, we have $P \approx 1$ mW for alcohol, $P \approx 15$ mW for water, and $P \approx 150$ mW for air. The temperature distribution in the stationary case does not coincide with the thermal-source distribution. However, as the shown in the calculations [13], at least for a thin medium the nonlocality of the process does not significantly affect the quality of the visualised image in such schemes, except for some increase in the edge sharpness, which occurs primarily for objects with sharp edges, the sizes of which are comparable with the illuminating-beam diameter. The experimental confirmation of this fact is presented in Fig. 4.

Figures 2a and 2b show visualised images of refractive-index fluctuations in glycerol caused by mechanical perturbations [20]. The image in Fig. 2b was obtained for a cell with an absorbing medium removed from the Fourier plane and, therefore, in the absence of self-imaging.

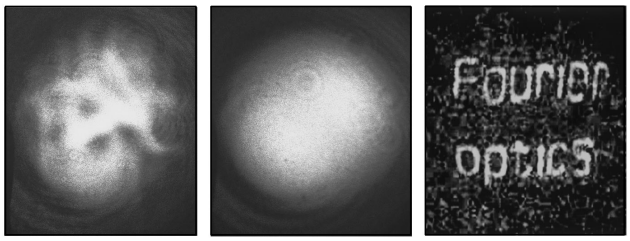

Figure 2. Visualised images of refractive-index fluctuations in glycerol, which were caused by mechanical perturbations (a) in the presence and (b) in the absence of self-imaging; (c) visualised image of a microscopic object.

Figure 2c presents a photograph of a visualised image of a phase microscopic object in the form of letters with a line thickness of 10 μm. Here, we used a weakly absorbing ($\alpha \simeq 2 \times 10^{-2}$ cm^{-1}), optically thick ($l \geqslant 100 l_{\text{d}}$) medium ($l_{\text{d}}$ is the diffraction length of the illuminating beam in the medium).

Figure 3 shows the self-imaging evolution for two crossed optical fibres placed in a cell with immersion oil. The image in Fig. 3a was obtained for the cell removed from the Fourier plane. Figures 3b and 3c demonstrate the self-imaging effect at laser powers of 1.2 and 3 mW, respectively. Figure 3c clearly reveals image inversion, with distortions caused by the thermal self-action of the beam in the medium. At a power $P \geqslant 5$ mW the beam broadening in the absence of the object can be seen well in the far zone. Thus, the main competing effect that impedes effective self-imaging is the thermal self-action of the illuminating beam in the absorbing medium.

Figure 3d demonstrates a visualised image of a phase object: edge of a Fresnel biprism. In this experiment self-

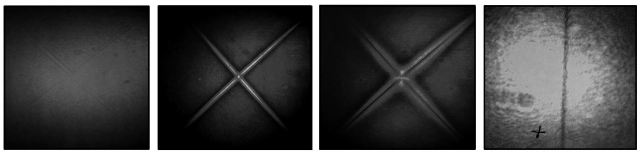

Figure 3. Images of two crossed optical fibres placed in a cell with immersion oil, (a) in the absence and (b, c) in the presence of self-imaging at laser powers of (b) 1.2 and (c) 3 mW; (d) a visualised image of an edge of a Fresnel biprism

imaging occurred in the light of a green laser pointer with a power of 25 mW in a cell 37 cm long, filled with unpurified (raw) water. The image 'development' time was few seconds.

We also investigated the quality of a visualised image of a transparent strip 120 μm wide. Its photograph and brightness distribution are shown in Fig. 4. One can see that self-imaging enhances the sharpness of object edges; this effect was theoretically predicted in [13]. It is also pronounced in the visualised images in Figs 3b and 3c.

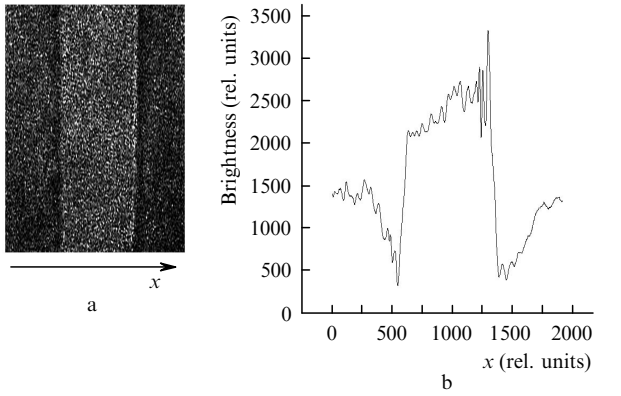

Figure 4. (a) Visualised image of a transparent strip and (b) the brightness distribution in it.

Thus, we presented the main characteristics of self-imaging of transparent objects and structures when spatially phase-modulated laser radiation is focused into a weakly absorbing medium. The required power level for effective imaging corresponds to the power in the initial stage of evolution of thermal self-action of illuminating laser beam; this is an important nonlinear optical phenomenon, which has the lowest threshold; it occurs during propagation of continuous and quasi-continuous laser radiation in natural media. Since self-imaging is independent of the angle of incidence of illuminating beam and of the position of the focal region in the medium, it can be implemented under the real atmospheric conditions even in the presence of thermal flows, which displace the beam waist as a whole in the Fourier plane. With allowance for the transformation linearity (in particular, in photothermal processes [5]), the schemes based on self-imaging can also be used in precise diagnostics and measurements of weak density fluctuations in gaseous (including plasma) media.

Acknowledgements. This study was supported by the grant of the President of the Russian Federation for the Support of Leading Scientific Schools (Grant No. NSh-4690.2006.2).

References

1. Born M., Wolf E. *Principles of Optics* (Oxford: Pergamon, 1969; Moscow: Nauka, 1973).
2. Francon M. *Fazovokontrastnyi i interferentsionnyi mikroskopy* (Phase-Contrast and Interference Microscopes) (Moscow: Fizmatlit, 1960).
3. Rytov S.M. *Usp. Fiz. Nauk*, **41** (4) 425 (1950).
4. Vorontsov M.A., Koryabin M.A., Shmal'gauzen V.I. *Upravlyaemye opticheskie sistemy* (Controlled Optical Systems) (Moscow: Nauka, 1988).
5. Babin A.A., Bubis E.L., Loshkarev V.V., et al. *Kvantovaya Elektron.*, **25**, 738 (1998) [*Quantum Electron.*, **28**, 804 (1998)]; Al'tshuller V.M., Bubis E.L., Shubin S.V. Preprint IAP RAS No. 241 (N. Novgorod, 1989).
6. Zharov V.P., Galitovsky V., Viegas M. *Appl. Phys. Lett.*, **83** (24), 4897 (2003).
7. Chernega N.V., Brekhovskikh G.L., Kudryavtseva A.D., et al. *Kvantovaya Elektron.*, **16**, 2530 (1989) [*Sov. J. Quantum Electron.* **19**, 1626 (1989)].
8. Vorontsov M.A., Justh E.W., Beresnev L.A. *J. Opt. Soc. Am. A*, **18**, 1289 (2001).
9. Komorowska K. et al. *J. Appl. Phys.*, **92**, 5635 (2002).
10. Trevino-Palacios C.G. et al. *Appl. Opt.*, **42**, 5091 (2003).
11. Bubis E.L. Preprint IAP RAS No. N698 (N. Novgorod, 2006).
12. Bubis E.L., Matveev A.Z. *Pis'ma Zh. Tekh. Fiz.*, **33** (11) 8 (2007).
13. Bubis E.L., Matveev F.Z. Preprint IAP RAS No. 737 (Nizhnii Novgorod, 2007).
14. Bubis E.L. *Pis'ma Zh. Tekh. Fiz.*, **34** (12) 29(2008).
15. Bubis E.L. *Prib. Tekh. Eksp.*, (1), 119 (2009).
16. Pushpa A.K. et al. *Appl. Opt.*, **48** (28) 5259 (2009).
17. Bubis E.L., Drobotenko V.B., Kulagin O.V., et al. *Kvantovaya Elektron.*, **15**, 147(1988) [*Sov. J. Quantum Electron.*, **18**, 94 (1988)].
18. Sukhorukov A.P. *Usp. Fiz. Nauk*, **101** (1), 81 (1971).
19. Smith D.K. *Trudy IIER*, **65** (12), 59 (1977).
20. Stebnovskii S.V. *Zh. Tekh. Fiz.*, **72** (11), 24 (2002).